Electronic Supplementary Information (ESI)

Two unprecedented entangled coordination polymers based on α-$\{SiW_{12}O_{40}\}^{4-}$

Yu-Hui Luo[a], Xiao-Yang Yu[a, b] and Hong Zhang[a]

[a] *Institute of Polyoxometalate Chemistry, Department of Chemistry, Northeast Normal University, Changchun, Jilin 130024, P. R. China*

[b] *College of Chemical and Pharmaceutical Engineering, Jilin Institute of Chemical Technology, Jilin City, Jilin, 132022, P. R. China*

* *E-mail: zhangh@nenu.edu.cn (H. Zhang)*

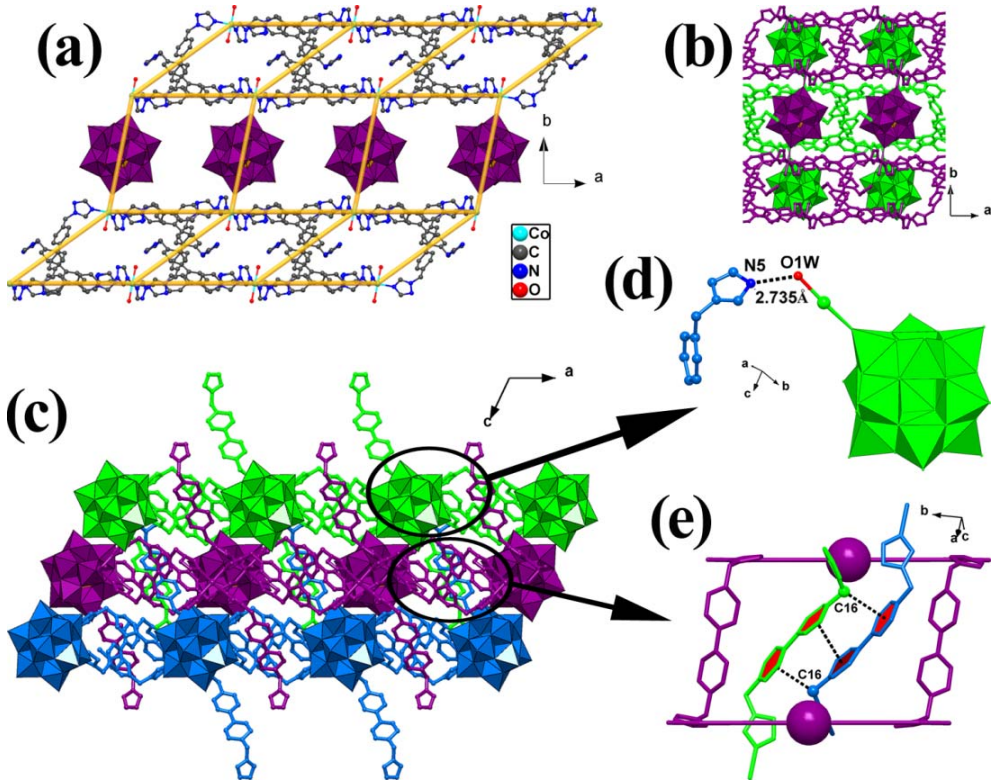

Fig. S1 (a) View of the 2D 4^4-**sql** layer of **1**. (b) The layers of **1** are alternately arranged in an *ABA* fashion. (c) View of 2D+2D→3D polypseudorotaxane structure of **1**. (d) Representation of O1W···N5 hydrogen-bonding interaction. (e) Illustration of $\pi\cdots\pi$ and C–H$\cdots\pi$ interactions (shown in black dashed line) between the mono-coordinated L ligands. The big purple balls in (e) represent $\{SiW_{12}\}^{4-}$ anions. All hydrogens are omitted for clarity.

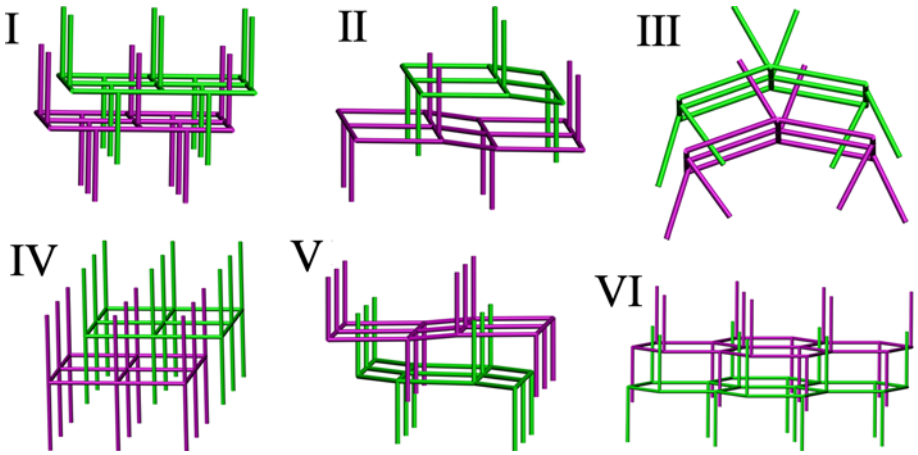

Scheme S1 Schematic representations of 2D+2D→3D polythreaded framework of compound **1** (**V**) and reported structures (**I-IV** and **VI**).

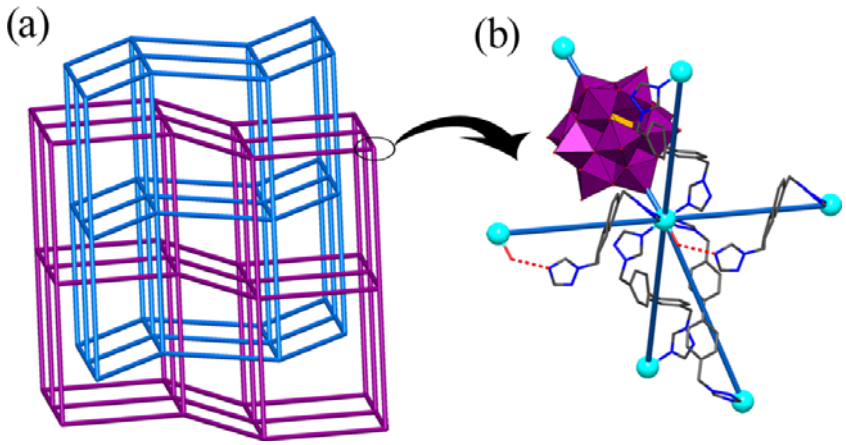

Fig. S2 (a) View of 2-fold **pcu** topological structure of **1**. (b) Schematic illustration of the 6-connected node based on O1W···N5 hydrogen bonds (shown in red dashed line). All hydrogens are omitted for clarity.

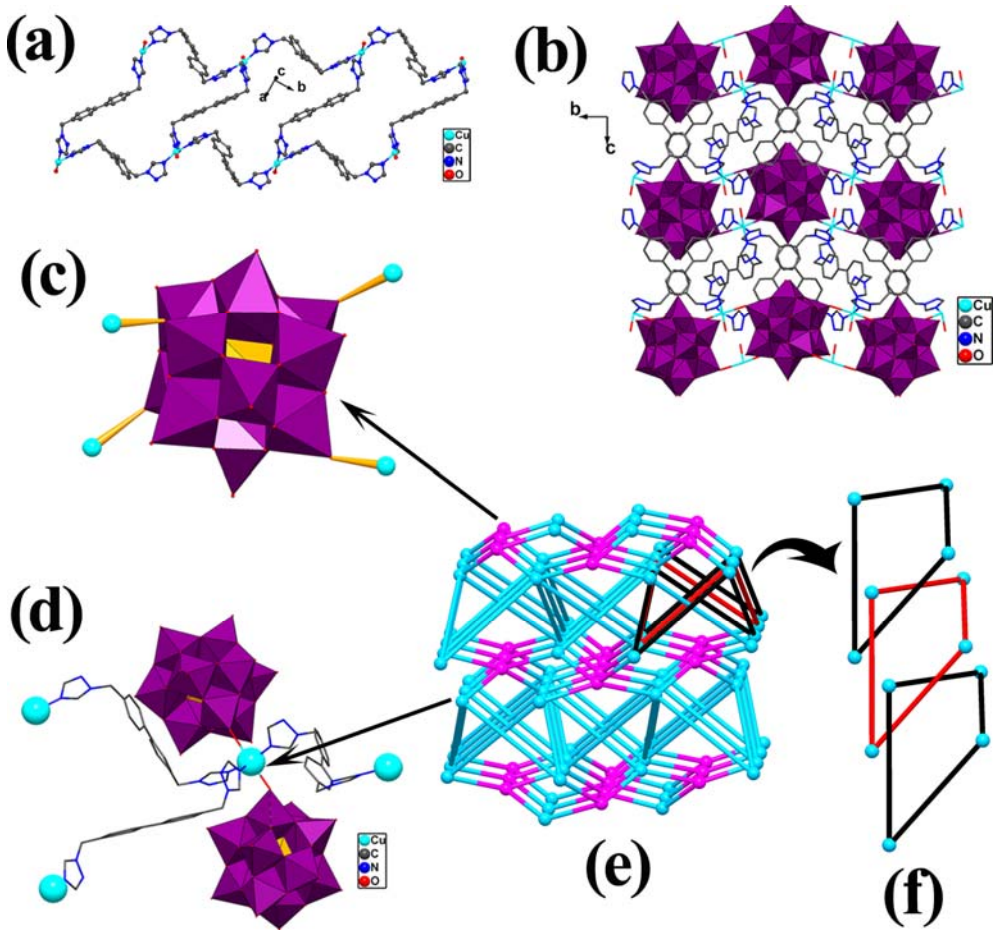

Fig. S3 (a) View of 1D ladder-shape chain of **2**. (b) Representation of 3D structure of **2**. (c) Illustration of 4-connected $\{SiW_{12}\}^{4-}$ anion. (d) Illustration of 5-connected Cu ions. (e) Topological view of **2**. The shortest interlocked 4-membered rings are highlighted in black and green. (f) View of self-catenated motif of **2**. All hydrogens are omitted for clarity.

Powder X-ray diffraction (PXRD) and thermal analysis. The PXRD patterns of **1** and **2** were measured at room temperature to check the purity of them. The peak positions of the tested PXRD patterns are in good agreement with the simulated patterns from their respective single-crystal data, suggesting the good phase purity of compounds **1** and **2** (Fig. S4).

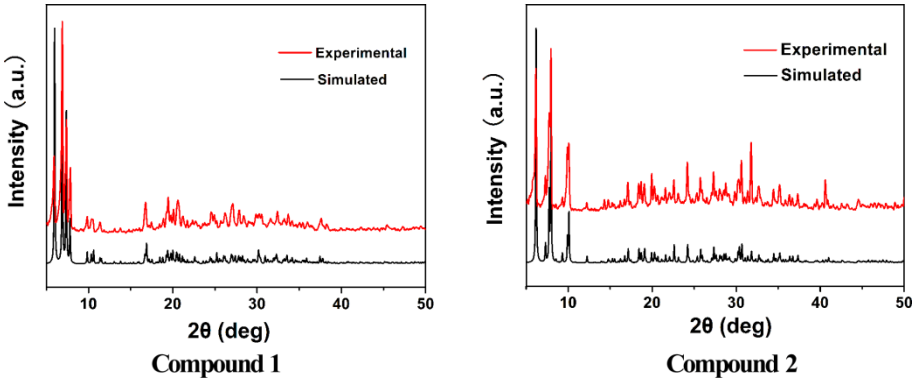

Fig. S4 The PXRD patterns of **1** and **2**.

The thermal stability of compounds **1** and **2** were investigated by thermogravimetric analysis (TGA) technique (Fig. S5). For **1**, the first weight loss from 160 to 190 °C corresponds to the release of lattice and coordinated water molecules (obsd 0.78 %, calcd 1.02 %). The further weight loss start from 360 °C may be attributed to the decomposing of the organic components. For **2**, similar decomposition behavior to that of **1** took place. The weight loss from 120 to 180 °C may be corresponds to the release of lattice and coordinated water molecules (obsd 1.42 %, calcd 1.35 %). The further weight loss from 350 to 570 °C attributed to the decomposition of the organic components.

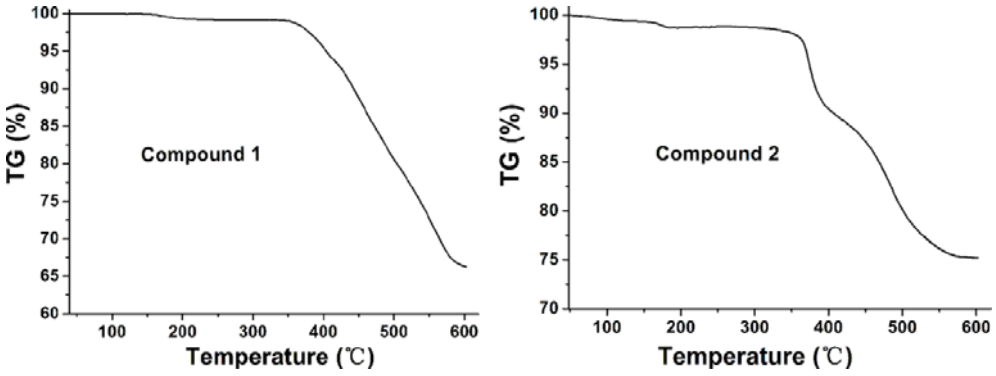

Fig. S5 Thermogravimetric analysis curves of **1** and **2**.

Solubility experiments. The samples of **1** and **2** were immersed in 60 °C solvents for 1 hour. The results show that both **1** and **2** are insoluble in water, methanol, ethanol, acetonitrile, acetone, ethyl acetate, cyclohexane, n-heptane, dichloromethane, trichloromethane and N,N-dimethylformamide.

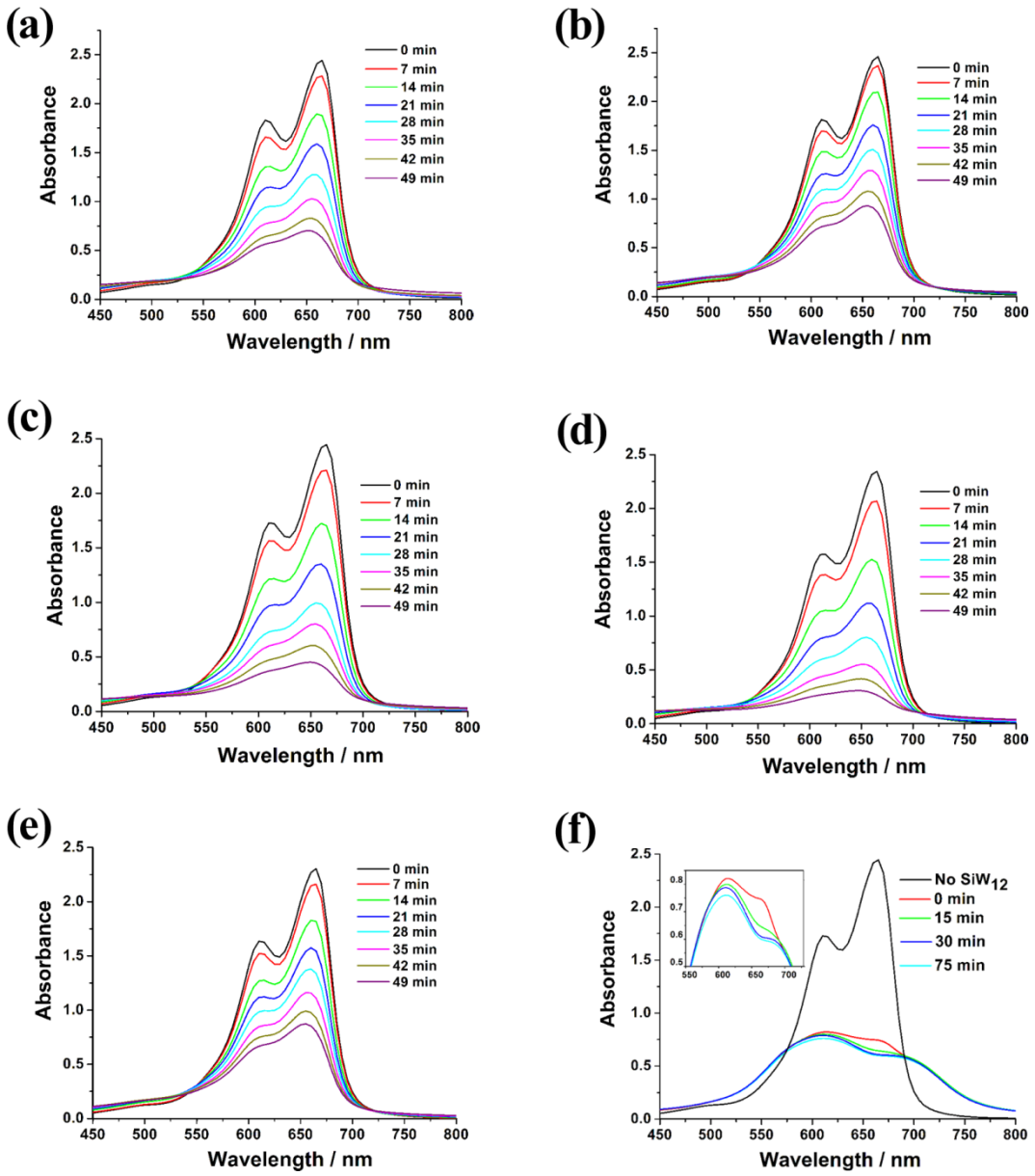

Fig. S6 Absorption spectra of the MB solution during the decomposition reaction under UV light irradiation with the presence of **1** (a), **2** (b), no catalyst (c), $CoCl_2 \cdot 6H_2O$ (d), $CuCl_2 \cdot 2H_2O$ (e) and SiW_{12} (f).

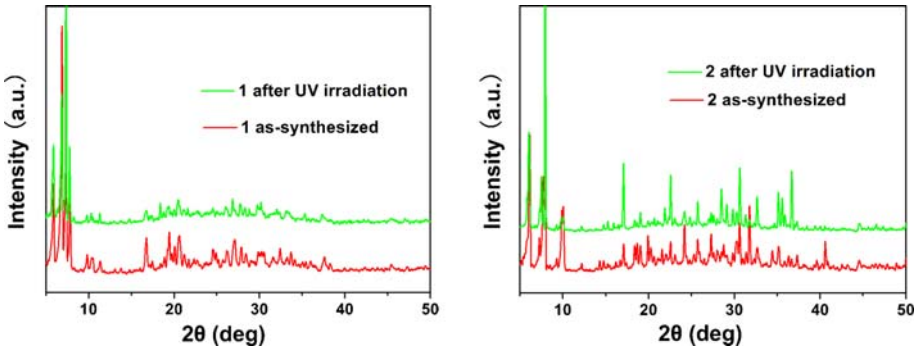

Fig. S7 The peak positions of the tested PXRD patterns of **1** and **2** after photocatalysis experiments are respectively in good agreement with those of the as-synthesized samples, indicating their high structural stability during the UV irradiation.

Table S1 Hydrogen-bonding geometry parameters for compound **1**.

D−H···A	d(D−H) (Å)	d(H···A) (Å)	d(D···A) (Å)	<(DHA) (°)
O1W···N5	--	--	2.735(3)	--

Table S2 C–H···π interactions in Compound **1**.[a]

C–H···π	Symmetry code	H–C(g) (Å)	X–H···C(g) (°)	X···C(g) (Å)
C(16)–H(16A)>Cg(2)	*1-x, 1-y, -z*	2.79	125	3.42(3)

[a]Cg(8):C(4)>C(5)>C(6)>C(7)>C(8)>C(9)

Table S3 π···π interactions in Compound **1**.[a]

Two rings	Cg-Cg (Å)	Alpha (°)	Gamma (°)	CgI_Perp (Å)	CgJ_Perp (Å)
Cg(10)>Cg(10)	3.892(2)	0	17.65	3.709(2)	3.709(2)

[a]Cg(10): C(10)>C(11A)>C(12A)>C(13)>C(14A)>C(15A); Alpha = Dihedral Angle between Planes I and J; Gamma = Angle Cg(I)>Cg(J) vector and normal to plane J; Cg-Cg = Distance between ring Centroids; CgI_Perp = Perpendicular distance of Cg(I) on ring J; CgJ_Perp = Perpendicular distance of Cg(J) on ring I.

Table S4 Selected bond lengths (Å) and angles (°) of **1**.

Co(1)–N(10)#1	2.068(18)	Co(1)–N(13)	2.136(14)
Co(1)–N(1)	2.092(16)	Co(1)–N(7)	2.122(19)
Co(1)–O(1W)	2.100(14)	Co(1)–O(5)	2.155(11)
N(10) #1–Co(1)–N(1)	96.3(7)	O(1W)–Co(1)–N(7)	89.3(7)
N(10) #1–Co(1)–O(1W)	88.0(6)	N(13)–Co(1)–N(7)	90.1(7)

N(1)–Co(1)–O(1W)	93.6(6)	N(10) #1–Co(1)–O(5)	87.6(6)
N(10) #1–Co(1)–N(13)	89.1(6)	N(1)–Co(1)–O(5)	86.4(6)
N(1)–Co(1)–N(13)	170.7(7)	O(1W)–Co(1)–O(5)	175.6(6)
O(1W)–Co(1)–N(13)	93.8(6)	N(13)–Co(1)–O(5)	86.3(5)
N(10) #1–Co(1)–N(7)	177.2(7)	N(7)–Co(1)–O(5)	95.1(7)
N(1)–Co(1)–N(7)	84.9(7)		

[a] Symmetry codes: #1, 1+*x*, *y*, *z*.

Table S5 Selected bond lengths (Å) and angles (°) of **2**[a].

Cu(1)–N(1)#2	1.95(2)	Cu(1)–N(7)	2.02(2)
Cu(1)–N(4)	1.98(2)	Cu(1)–O(18)	2.301(17)
Cu(1)–O(1W)	2.03(2)	Cu(1)–O(10)#1	2.652(2)
N(1) #2–Cu(1)–N(4)	167.0(10)	N(4)–Cu(1)–O(18)	97.9(8)
N(1) #2–Cu(1)–O(1W)	90.2(10)	O(1W)–Cu(1)–O(18)	86.2(8)
N(4)–Cu(1)–O(1W)	87.2(9)	N(7)–Cu(1)–O(18)	90.2(8)
N(1) #2–Cu(1)–N(7)	93.5(11)	O(10)#1–Cu(1)–N(7)	93.2(6)
N(4)–Cu(1)–N(7)	90.0(10)	N(4)–Cu(1)–O(10)#1	81.0(4)
O(1W)–Cu(1)–N(7)	175.1(9)	O(1W)–Cu(1)–O(10)#1	86.3(6)
N(1) #2–Cu(1)–O(18)	94.6(8)	O(10)#1–Cu(1)–O(18)	176.4(2)
N(1) #2–Cu(1)–O(10)#1	86.3(4)		

[a] Symmetry codes: #1, 1/2+*x*, 1−*y*, 1/2−*z*; #2, 1/2+*x*, 1/2+*y*, −*z*.